RSC Sustainability

ROYAL SOCIETY OF CHEMISTRY

PAPER

View Article Online
View Journal | View Issue

Cite this: *RSC Sustainability*, 2025, **3**, 440

Unveiling the sustainable oxidation approach of homologous alcohols by DPA in a CTAB micellar environment†

Sandip Kundu, ‡[a] Mandira Mitra, ‡[a] Priya Karmakar,[a] Sk Mehebub Rahaman,[a] Mousumi Layek,[a] Pintu Sar *[ab] and Bidyut Saha *[a]

Received 24th September 2024
Accepted 19th November 2024

DOI: 10.1039/d4su00593g

rsc.li/rscsus

This study explores the catalytic oxidation of homologous alcohols (2-propanol, 2-butanol, and 2-pentanol) by the diperiodatoargentate(III) (DPA) complex in a cetyltrimethylammonium bromide (CTAB) micellar medium. Notably, the use of a micellar medium avoided the need for organic solvents, aligning with green sustainable chemistry principles. The reaction kinetics were monitored by UV-vis spectroscopy, tracking the reduction of Ag(III) to Ag(I) at 360 nm. For all three alcohols, the maximum rate augmentation is observed at a 5 mM CTAB concentration. Zeta potential measurements supported the significant enhancement in reaction rate of the studied reactions in a micellar medium. NMR, DLS, and UV-vis studies revealed interactions between CTAB and DPA. A bathochromic shift is observed in the UV-vis study in the region of 0.8–2 mM CTAB concentrations in the CTAB–DPA system. The critical micelle concentration (CMC) of CTAB was evaluated in the presence of DPA, demonstrating its impact on micelle formation. This green catalytic system demonstrates promising efficiency and sustainability for alcohol oxidation reactions, with potential applications in organic synthesis and industrial processes.

Sustainability spotlight

Aqueous cationic micellar systems, formed by self-assembling cetyltrimethylammonium bromide (CTAB), serve as a green catalytic platform, enabling the efficient and selective oxidation of homologous alcohols with diperiodatoargentate(III) (DPA) as an environmentally benign oxidant. This sustainable approach facilitates selective transformations, minimizing waste and environmental impact. By leveraging micellar catalysis, this method reduces the need for harsh chemicals and energy-intensive processes, promoting a more environmentally friendly and cost-effective solution for chemical synthesis.

1 Introduction

Natural processes that involve the chemical synthesis of different organic compounds take place in aqueous media along with a high value of atom economy, signifying that such processes are green and have no adverse effects on the environment. A chemical synthesis process must comply with all twelve green chemistry principles, whether it is carried out on a small scale in a lab or on a large scale in industry.[1] Following the path of nature, increasing interest in the use of water as a solvent for organic transformations has been continually helping to recuperate the environment.[2,3] Hailes *et al.* focused on the selection of alternative solvents for organic transformations, which usually proceed in conventional volatile organic solvents like CH_2Cl_2, Me_2N–CHO, $Me_2S{=}O$, *etc.*[4] According to the "like dissolves like" rule, it is inevitable that organic compounds do not dissolve in water. In this context, the micellar microenvironments produced by certain concentrations of surfactants in water appear to be a perfect remedy to the insolubility problem of organic molecules in water.[5] Micelles are self-assembled nanostructures of surfactants that have numerous advantages in organic synthetic chemistry, such as easy solubilisation of water-hating substrates, excellent encapsulation of organic molecules, driving the organic reaction in a nano-dimensional micro-reactor, promoting the reaction rate, *etc.* Even though the improvement in reaction rate is determined by the surface charge of the micelles. Depending on the charge of the head group, different kinds of surface-active agents are available.[6] The structural diversity of cationic surfactants is really worth mentioning; additionally certain biological (*e.g.* drug carriers)[7] and nano-technological applications (*e.g.* antibacterial and bioimaging agents, supramolecular catalysts, stabilizers of nanoparticles) make them suitable candidates for numerous prime applications.[8] The cationic

[a]*Surfactant Chemistry Laboratory, Department of Chemistry, The University of Burdwan, Burdwan-713104, West Bengal, India. E-mail: pintusar1@gmail.com; b_saha31@rediffmail.com; bsaha@chem.buruniv.ac.in*

[b]*Department of Chemical Science, Indian Institute of Science Education and Research, Kolkata-741246, West Bengal, India*

† Electronic supplementary information (ESI) available. See DOI: https://doi.org/10.1039/d4su00593g

‡ Sandip Kundu and Mandira Mitra are joint first authors.

surfactant cetyltrimethylammonium bromide (CTAB), with a quaternary ammonium head group, offers many advantages when it coexists with oppositely charged substances. These formulated catanionic conjugated systems are stabilized by electrostatic forces of attraction.[9,10] Thus, aqueous CTAB-mediated chemical transformations are an interesting topic of research that is still being explored with a focus on elucidating their applications in sustainable catalysis, green chemistry, and environmentally benign synthesis.[11]

While talking about micelle-mediated chemical transformations, several groups, including ours, have long been involved in elucidating the impact of nano micellar media in promoting the oxidation reaction kinetics.[12–14] Hitherto, the oxidizing ability of transition metal ions at high oxidation states is familiar on account of their strong affinity to snatch electrons from other substrates. For example, vanadium(v),[15] chromium(vi),[16] manganese(vii),[17] cerium(iv),[18] and iron(iii)[19] metal ion-directed oxidative transformations in micellar microenvironments have been thoroughly investigated. However, employing these metals to execute oxidative transformations requires a number of harsh conditions, such as an excessively high or low pH, high temperature, *etc.* In order to prevent the aforementioned situation, silver(iii), and likewise copper(iii),[20] is employed as an oxidising agent in the present study. Herein, we focus on the effectiveness of diperiodatoargentate(iii) (DPA) as an oxidising agent for the oxidation of aliphatic alcohols within a green envelop generated by an aqueous-CTAB medium. In addition to this, the interaction study between CTAB and Ag(iii) ion (DPA) is truly crucial because of the favourable conjugation between them. The selection of analogous aliphatic alcohols (secondary) as the substrate for the present kinetic study of the Ag(iii)-directed oxidation process is quite interesting in order to get a better understanding of the kinetic profiles in CTAB-micellar microenvironments. In spite of that, the single step oxidation of such secondary alcohols (propan-2-ol, butan-2-ol, pentan-2-ol) produces some industrially important organic ketonic compounds, like acetone, butan-2-one, and pentan-2-one, respectively, which are mostly utilised in the personal care business and pharmaceutical industry as a solvent, textile industry as a removal agent, petroleum industry as a fuel additive, precursor to vitamin E, and many others. Our main objective is to investigate the CTAB-mediated oxidation kinetics of the aforementioned alcohols following mechanistic aspects of micellar media and surfactant–oxidant interactions.

2 Materials and methods

2.1. Reagents used

Potassium hydroxide (SRL, India, AR), silver nitrate (Merck, India, AR), potassium persulfate (Merck, India, AR), sodium hydroxide (SRL, India, AR), potassium periodate (Merck, India, AR), cetyltrimethylammonium bromide (CTAB) (SRL, India, AR), propan-2-ol (Merck, India, AR), butan-2-ol (Merck, India, AR), pentan-2-ol (Merck, India, AR), and pyrene (SRL, India, AR) were used. Double distilled water with a specific conductance value from 1–2 S cm^{-1} was employed to prepare all of the reaction mixtures. All other commercially available chemical substances were obtained in their purest form.

2.2. Instrumentation

A UV-vis SHIMADZU-1800 spectrophotometer with a SHIMADZU, TCC-controller was used to monitor the oxidation kinetics. The above spectrophotometer was used also for measuring the strength of the synthesized Ag(iii) periodate complex. The ^{1}H NMR analysis was carried out using a Bruker ASCEND-400 MHz spectrometer to explore the localization of substrate molecules in the micellar microenvironment; additionally, the oxidised product was identified with a ^{1}H NMR spectrometer. An FT-IR (PerkinElmer) study also helped to confirm the corresponding oxidized product for every studied reaction using a variety of substrates. A Hitachi FL-7000 Spectrofluorometer was used to measure the steady state fluorescence. The electrical conductivities of the surfactant solutions were measured using a conductometer (Eutech Instrument PCD 6500) having a cell constant of 1 cm^{-1}. Zeta potential measurements and DLS studies were carried out using Malvern Zetasizer Nano ZS-90 apparatus with a capillary cell.

2.3. Procedure of the preparation of the Ag(iii)-periodate complex

The conventional synthetic procedure of silver(iii) periodate (DPA) from literature reports helped us to synthesize the complex.[21] Following this procedure, KOH (14 g) and KIO_4 (11.5 g) were added in a 50 mL $AgNO_3$ (4.25 g) solution and the mixture was just heated to boiling in a heating mantle. Afterward, 10 g of $K_2S_2O_8$ was added and the whole mixture was allowed to stand during cooling. A porous fitted glass filter was used to filter the solution. Following this, approximately 20 g of NaOH was added continuously until a significant amount of orange precipitate appeared. Next the precipitate was filtered using the above set up and rinsed with cold water several times. Some crystals appeared and these were dissolved in water and the solution was heated up to 80 °C with continuous stirring. Some of the solid particles were dissolved forming a dark red coloured solution. The final product was filtered, cooled and diluted to the volume of 100 mL. In compliance with Lambert–Beer's law, an appropriate dilution of the DPA stock solution was prepared for the UV-visible study.

2.4. Kinetic procedure

The kinetics of the studied reaction were investigated by measuring the change in the absorbance of Ag(iii) at the 360 nm wavelength with respect to time, as the other components do not absorb profoundly at this wavelength. During the kinetic study, the oxidant concentration was kept fixed at 5.5×10^{-5} M and the surfactant concentration varied, while the concentration of the substrates was maintained at least 15 times greater than the concentration of DPA (pseudo first order conditions), *i.e.*, to make the reaction first order with respect to the substrate (here alcohol). After completion, silver(iii) is reduced to silver(i) indicating that this is a two electron transfer oxidation process. The lowering of the absorbance value at 360 nm observed at

regular time intervals has been monitored through a spectrometric approach. All of the reaction kinetics have been followed up to 80% completion and from the plot of $-\ln(\mathrm{Abs})_{360}$ *vs.* time, the kinetic profile of oxidation has been analyzed. The slope of the aforementioned plot (straight line) was used to calculate the observed rate constant (k_{obs}) of the corresponding reaction. The half-life period ($t_{1/2}$) was calculated using the formula $t_{1/2} = \ln 2/k_{obs}$. The kinetics of the reactions were also studied at pre-micellar, near micellar and post micellar concentrations to investigate the effect of the CTAB surfactant on the reaction rate profile.

2.5. Product analysis

The oxidised products of each substrate were isolated from the corresponding reaction mixture using the solvent extraction method, followed by the fractional distillation approach. The extracted product was treated with a freshly prepared saturated solution of 2,4-dinitrophenylhydrazine in 2(M) acidic solution in order to ensure the formation of the carbonyl product. The yellowish orange precipitates of hydrazone derivatives were dried and further used for FT-IR studies.

3 Results and discussion

3.1. Structural characterisation of the synthesised complex

In accordance with the reports in the literature, we have synthesised the Ag(III) periodate complex in alkaline media. In the solution phase, the colour of the Ag(III) periodate complex was found to be reddish yellow. Three absorbance bands at 208 nm, 252 nm, and 360 nm appeared in the UV-vis spectrum of the synthesised complex (Fig. 1), and among them the peak at 360 nm suggests the existence of a Ag(III) periodate complex.[22] A broad stretching vibration at around 3500–3200 cm^{-1} was noticed in the FT-IR spectrum (Fig. 1), indicating the presence of an O–H bond, whereas the band at 1635 cm^{-1} is attributed to the (HOH) bending mode. The moderate intensity bands at 2305 cm^{-1} and 2115 cm^{-1} may be the result of ϑ(OH) stretching of strongly hydrogen-bonded moieties. The bending vibration mode of δ(IOH) appeared at around 1400 cm^{-1}. The FT-IR frequencies at 800–700 cm^{-1} and 500–400 cm^{-1} correspond to the stretching vibrations of ϑ(I=O) and ϑ(AgO), respectively. The observed spectroscopic results are in good agreement with the prior literature report.[23] The successful synthesis of the Ag(III) periodate complex following thorough characterization makes it possible to employ DPA in the kinetic investigation. Ultimately, following Lambert–Beer's law, the absorbance value at 360 nm wavelength is used to calculate the strength of the DPA solution (the molar extinction coefficient 'ε' at 360 nm is 13 900 ± 100 $dm^3\ mol^{-1}\ cm^{-1}$).[24] Prior to the comprehensive kinetic study, we should have knowledge about the aqueous chemistry of Ag(III) species or DPA complexes in alkaline media.

3.2. Aqueous chemistry of the Ag(III) periodate complex

As accounted in numerous reports, the water soluble DPA has a square planar structure with the formula $[Ag(IO_6)_2]^{7-}$; however, in an alkaline medium it doesn't exist in the same

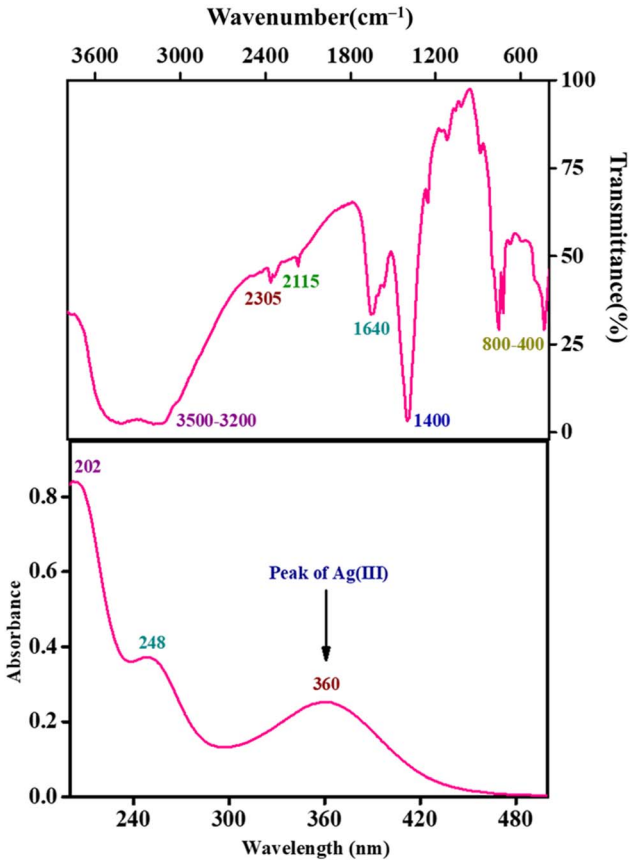

Fig. 1 UV-vis scan and FTIR profile of the synthesised DPA complex.

form. The periodate species is believed to have subsequent forms depending on the pH of the solution shown below in eqn (1)–(3). The dominating species eventually loses one proton each time as the pH of the medium moves towards the alkaline state to create another deprotonated substrate.[25]

$$H_5IO_6 \rightleftharpoons H_4IO_6^- + H^+ \quad (1)$$

$$H_4IO_6^- \rightleftharpoons H_3IO_6^{2-} + H^+ \quad (2)$$

$$H_3IO_6^{2-} \rightleftharpoons H_2IO_6^{3-} + H^+ \quad (3)$$

The main species of the periodic acid is H_5IO_6 in acidic medium and in neutral medium the major species is $H_4IO_6^-$. The present reaction conditions are alkaline; hence, the active species of the periodic acid is $H_3IO_6^{2-}$. It has also been reported that the periodate has a tendency to form a dimer at higher concentration (Fig. 2).[26]

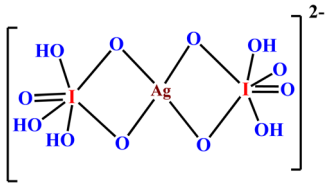

Fig. 2 Structure of DPA.

Table 1 The experimentally determined CMC value and counterion binding parameter of CTAB in the absence and presence of reactant molecules

	CMC (fluorometric)	CMC (conductometric)	β	ΔG°_{mic}(kJ mol^{-1})
CTAB	1.03	0.98	0.559	−24.49
CTAB + DPA	0.85	0.86	0.315	−20.15
CTAB + propan-2-ol	1.68	1.71	0.318	−18.88
CTAB + butan-2-ol	1.57	1.51	0.152	−16.86
CTAB + pentan-2-ol	1.27	1.25	0.203	−18.72

[Alcohol] = 8.3×10^{-4} mol dm^{-3}, [DPA] = 5.5×10^{-5} mol dm^{-3}

With a reduction potential of 1.74 V, DPA appeared as a vigorous oxidising agent in an aqueous alkaline medium, offering numerous selective organic transformations in micellar media also.[27] Before uncovering the kinetic profiles of oxidation of isomeric secondary alcohols in micellar media, it is necessary to highlight the interaction of the surfactant with the reactant molecules.

3.3. CMC and interaction study of the surfactant

The formulation of a variety of self-assembled nanostructures by the commercially available surfactants above their CAC (critical aggregation concentration) in aqueous solution is a well-recognized fact.[28,29] To validate the aggregation of the CTAB surfactant, we have measured the micellization concentration (*i.e.*, CMC) using conductometric and fluorometric methods (Table 1). It is noticed that the CMC of CTAB alone in aqueous media is close to 1. These experimentally measured CMC values are in good agreement with the literature reports.[30] In order to realize the impact of alcohols (2-propanol, 2-butanol, and 2-pentanol) on the aggregation of CTAB, we measured the CMC of CTAB in several microenvironments (Fig. S3 and S4†). The presence of such alcohols elevated the CMC value of CTAB from 1.03 to 1.27, 1.57, and 1.68 mM for 2-propanol, 2-butanol, and 2-pentanol, respectively, indicating that an alcoholic medium does not favour the self-association of CTAB monomers. Nevertheless, the CMC of CTAB drastically fell in the presence of DPA nearly in the range of 0.86 mM (Fig. 3), indicating strong interaction of the CTAB with the oxidant DPA molecule favouring micelle formation. This could be because the strong electrostatic attraction between the positively charged ammonium head group of CTAB and the negatively charged DPA species drives the micellization of CTAB.

We analyzed the interactions between the surfactant tail and the alcohols on the basis of the binding parameter (β) to show the strength of hydrophobic effects upon micellization. In general, the hydrophobic influences among the surfactant tail groups are the key driving factor behind the micelle formation. Because of the strong interaction between the surfactant tail group and the hydrophobic portion of the alcohols, hydrophobic molecules are highly solubilized in alcoholic solutions, which disfavours the micellization process. This phenomenon is emphasized by the elevated CMC value of CTAB in the presence of alcohols, which also correlates with the prior study.[31]

The following equation has been used to compute the thermodynamic parameter (free energy of micellization) for the surfactant alone, the surfactant in the presence of the oxidising agent DPA and the alcohols, separately.[32]

$$\Delta G^{\circ}_{mic} = (1+\beta)RT \ \ln X_{CMC} \quad (4)$$

The X_{CMC} stands for the CMC of the micelle in mole fraction units and β is the counter-ion binding parameter, calculated by subtracting the counterion dissociation (α) from unity. Herein, the counterion dissociation is calculated from the ratio of two slopes of conductivity plots (Fig. S2 and S3†).[33] The β values fall down in the mixture compared to pure CTAB micelles, which is a sign of the lowering of the effective surface charge density in

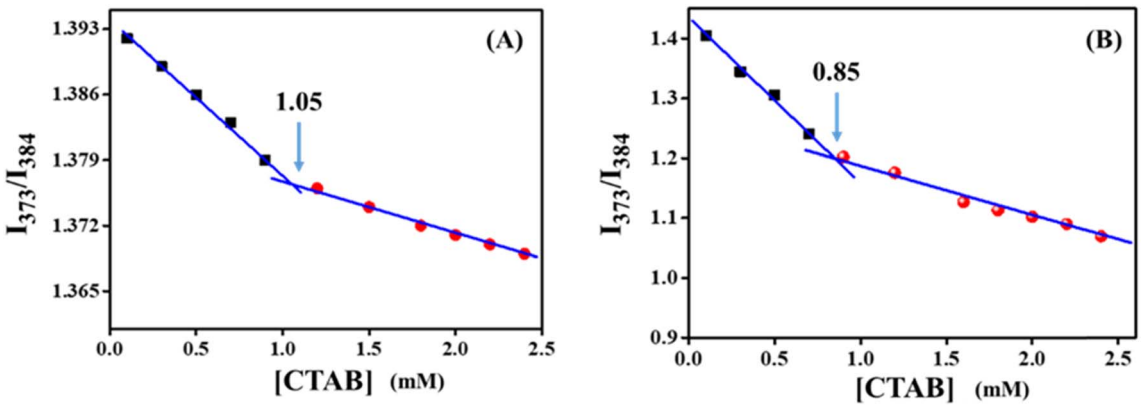

Fig. 3 Determination of the CMC of CTAB in the pure state (A) and in the presence of DPA (B).

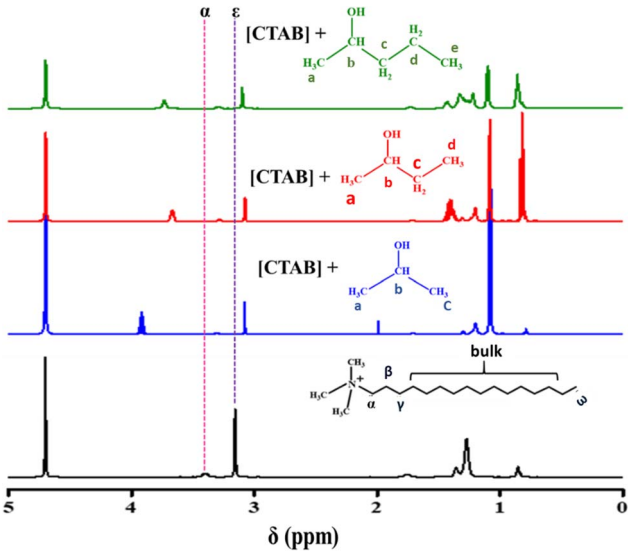

Fig. 4 ^{1}H NMR spectral shift (in D_2O) providing evidence of the incorporation of the substrate molecules in the CTAB micellar aggregates.

the presence of DPA or the substrate (alcohols). When the pure CTAB micelles are associated with the negatively charged DPA species, a strong electrostatic force of attraction operates between them. As a result, the DPA molecules displace some Br^- ions from the head group of the surfactants in the micelle's stern layer. This could be evidenced by the shift in wavelength dependent on the concentration of the surfactant. In contrast, the hydrophobic section of alcohols is likely to be in the palisade layer of the CTAB micelle, while the –OH group tends to orient toward the stern layer region as substantiated through NMR study.

To understand the solubilisation of alcohols in a CTAB micellar microenvironment, we have performed the ^{1}H NMR study of CTAB only and CTAB with different alcohols, separately (Fig. 4). As noticed, the chemical shift (δ) value of the α protons of CTAB shifts towards the upfield area when the aforementioned alcohols were present in the micellar medium. This finding suggests that there is some crowding of electrons experienced by the protons located on the C-atom immediately next to the N-atom of the CTAB molecule. Again, the ε proton of the CTAB molecule shifts to some extent towards the upfield region, which is a clear indication of increased electron density around that proton. In the presence of the studied alcohols, the other protons, *viz.* β,γ, bulk and ω protons, of the CTAB molecule do not shift so much in comparison to the proton of the

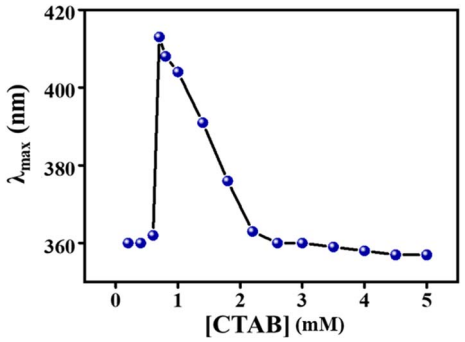

Fig. 5 Variation of the λ_{max} (nm) of DPA with varying CTAB concentration (mM).

pure CTAB molecule. The comparable chemical shift values of the CTAB protons in the presence of alcohols indicate that the alcohols are likely to be solubilised in the close proximity of the quaternary ammonium moiety, *i.e.*, surfactant head groups (Table 2).

In order to understand the significant interaction between CTAB and DPA species, we have performed UV-vis study for which a set of samples were prepared keeping the concentration of DPA constant (5×10^{-5} mol dm^{-3}) whilst varying the CTAB concentration from below to above the CMC. The characteristic peak of silver(III) appeared at 360 nm; however, a bathochromic shift is observed when the concentration of CTAB varies from 0.8 mM to 2.0 mM. As noticed from conductometric measurements, the cationic CTAB surfactant usually forms micelles at concentrations around 1.0 mM. Herein, it should be remembered that the interactions that drive the micellization process are: hydrophobic attraction among the tails of the surfactants and electrostatic repulsion between the head groups of the surfactants. Another important point needs to be considered for micelle formation in aqueous media is the binding of counter ions.[34] Here, the Ag(III)-species is negatively charged; thus, it is attracted by the quaternary ammonium moiety of CTAB through electrostatic force of interaction. As a result, the generation of micellar nanoaggregates is significantly influenced when DPA is introduced to the medium. This crucial electrostatic force may begin to operate when the [CTAB] is 0.7 mM, which can be supported by the extensive jump of λ_{max} value from 360 nm to 415 nm near the micellization concentration of CTAB (Fig. 5). Afterward, the λ_{max} value decreases as the CTAB concentration increases up to 2.0 mM, and then levels-off. In summary, the appearance of a bathochromic shift in the presence of DPA has been observed in the CTAB concentration range of 0.8 mM to 2.0 mM. Beyond that the λ_{max} value does not alter with the rise

Table 2 ^{1}H NMR chemical shift (ppm) values (all the solutions are prepared in D_2O solvent)

	α	β	γ	Bulk	ω	ε	*a*	*b*	*c*	*d*	*e*
CTAB	3.381–3.423	1.757	1.356	1.272	0.836–0.866	3.157	—	—	—	—	—
CTAB + 2-propanol	3.289–3.317	1.704	1.299	1.199	0.778–0.801	3.078	1.075–1.086	3.890–3.952	1.992	—	—
CTAB + 2-butanol	3.247–3.317	1.70–1.75	1.307	1.20	0.787–0.799	3.076	1.08–1.09	3.6–3.7	1.353–1.450	0.809–0.834	
CTAB + 2-pentanol	3.280–3.307	1.729	1.255–1.329	1.219	0.821	3.098	1.097–1.108	3.719–3.748	1.338–1.474	1.338–1.474	0.847–0.870

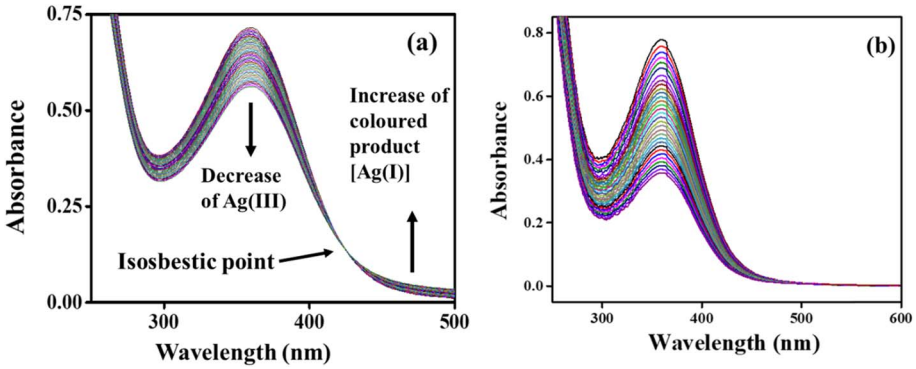

Fig. 6 Absorption spectra of the oxidation reactions of 2-butanol by DPA in aqueous media at $T = 30$ °C (a) in the absence of CTAB at regular 3 min intervals and (b) in the presence of 5 mM CTAB at regular 1 min intervals. [Conditions: [DPA] = 5.5×10^{-5} mol dm^{-3}; [CTAB] = 5.0 mM; [2-butanol] = 8.3×10^{-4} mol dm^{-3}].

of CTAB concentration. Because of the reduced intensity of the electrostatic interaction after 2.0 mM concentration of CTAB, the bathochromic peak has practically disappeared. It is widely known that this specific red shift results from the interaction of the cationic surfactant with the anionic moiety.[35]

3.4. Kinetic analysis of the studied reactions in a micellar microenvironment

The progress of the oxidation kinetics was monitored by the spectrophotometric method following the time dependent reduction of the absorbance value at 360 nm. All three analogous alcohols were used for the oxidation study to get an insight into the chain length-dependent kinetic profile. In aqueous media only, the observed rate constants, k_{obs} (s^{-1}) are 0.183×10^{-4}, 0.265×10^{-4}, and 0.198×10^{-4} for 2-propanol, 2-butanol, and 2-pentanol, respectively. Fig. 6a presents the progress of the oxidation kinetics of 2-butanol in the absence of surfactant. A rapid drop of absorbance at 360 nm wavelength is observed when CTAB is introduced into the reaction media (Fig. 6b). This drop of absorbance is similar for 2-propanol (Fig. S5†) and 2-pentanol (Fig. S6†). When the reaction proceeds without surfactant medium, a well-defined isosbestic point is observed at 415 nm (Fig. 6a). This indicates the formation of a transient DPA-complex where the absorbance of the two species remains unchanged. After the isosbestic point, a small peak of colored compound [Ag(I)] was noticed in the studied region. In this work, we have used aqueous cetyltrimethylammonium bromide ($CTA^+ Br^-$) as the reaction medium. Herein, after the reduction of Ag(III), the reduced species, Ag^+ ions, have the tendency to attach with the counterion of the surfactant (Br^-), and hence silver bromide is formed in the reaction medium. This may be the reason for the disappearance of the isosbestic point when the reaction proceeds with aqueous surfactant medium (Fig. 6b). It is worth mentioning that the mechanism of the electron transfer process remained unchanged when we introduced CTAB as the reaction medium.

On assessment of Table 3, the micellar medium speeds up the reaction rate as compared to the case without surfactant–micelle medium for each of the alcohols. Following the earlier study of micelle-mediated reaction kinetics, we have evaluated the oxidation rate at various [CTAB] ranges from the pre- to post-micellar region. The data of k_{obs} values in Table 3 are described by second-order polynomial equations with an intercept equal to 0 for all three alcohols. The equations below represent the general equations used to observe the dependence of k_{obs} with the concentration (CTAB) for three different alcohols.

$$k_{obs} \times 10^4 = 0 + (0.05314 \pm 0.43425)C + (0.27722 \pm 0.10383)C^2, \text{[for 2-propanol]} \quad (5)$$

$$k_{obs} \times 10^4 = 0 + (0.79771 \pm 0.32552)C + (0.00734 \pm 0.07783)C^2, \text{[for 2-butanol]} \quad (6)$$

Table 3 The observed rate constant (k_{obs}) and half-life ($t_{1/2}$) of the studied reactions in the presence of a micellar microenvironment

Substrate	CTAB (mM)	$10^4 \times k_{obs}$ (s^{-1})	$t_{1/2}$ (h)
2-Propanol	0	0.183	10.52
	0.6	0.820	2.35
	0.8	1.451	1.33
	1	0.983	1.96
	2	0.792	2.43
	3	1.637	1.18
	4	4.668	0.41
	5	7.550	0.25
2-Butanol	0	0.265	7.26
	0.6	0.863	2.23
	0.8	1.647	1.17
	1	1.075	1.79
	2	0.713	2.70
	3	2.335	0.82
	4	3.497	0.55
	5	4.2	0.46
2-Pentanol	0	0.198	9.72
	0.6	0.635	3.03
	0.8	0.895	2.15
	1	0.995	1.93
	2	0.885	2.17
	3	1.318	1.46
	4	1.833	1.05
	5	3.012	0.64

[Conditions: [alcohol] = 8.3×10^{-4} mol dm^{-3}, [DPA] = 5.5×10^{-5} mol dm^{-3} at 30 °C]

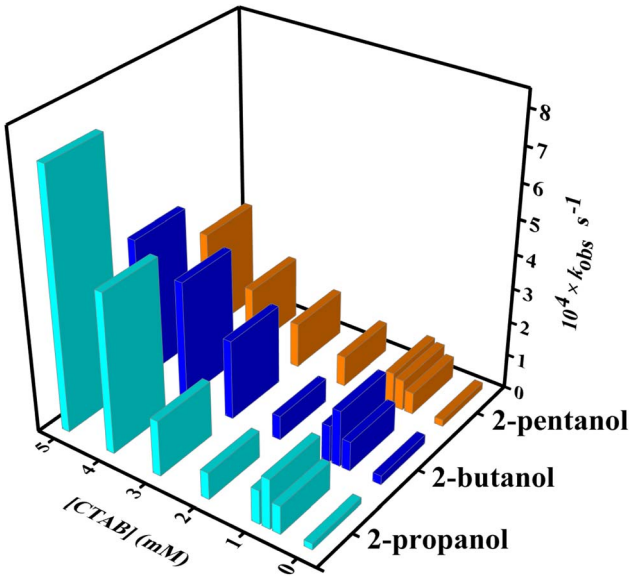

Fig. 7 Comparative analysis of the rate constants of the studied reactions with varying concentration of CTAB.

$$k_{obs} \times 10^4 = 0 + (0.53583 \pm 0.20679)C + (8.9385 \times 10^{-4} \pm 0.04944)C^2, \text{ [for 2-pentanol]} \quad (7)$$

Here, C is the concentration CTAB. The k_{obs} value increases from the beginning after the addition of CTAB into the reaction medium and this increment of k_{obs} has been noticed up to 0.8 mM [CTAB] for all three alcohols (2-propanol: 1.451×10^{-4}, 2-butanol: 1.647×10^{-4}, 2-pentanol: 0.895×10^{-4} s^{-1}). Afterward, a little fall in k_{obs} value has been observed for the oxidation of 2-propanol (0.792×10^{-4} s^{-1}), 2-butanol (0.713×10^{-4} s^{-1}), and 2-pentanol (0.885×10^{-4} s^{-1}) until [CTAB] ~2 mM (Fig. 7). The usual enhancement of the reaction rate for the DPA oxidation of alcohols in CTAB micellar media can be demonstrated in the light of solubilization of reactants in a micellar microenvironment. Certainly, the CTAB medium in the concentration range of 0.8 mM to 2.0 mM fails to promote the reaction rate due to the disorganized aggregation of CTAB. The CTAB molecules feel a twisting situation in the range of 0.8 mM to 2.0 mM since DPA species favour the micellization of CTAB, while alcoholic substrates disfavour the formulation of nanomicelles. The bathochromic shift of λ_{max} for the binding of DPA to the CTA^+ ions is also an indication of the chaotic micellization of CTAB. Probably, this results in the slight diminishing of the k_{obs} value for the CTAB-mediated reaction in the concentration range of 0.8 mM to 2.0 mM. In order to provide potential evidence of the inconsistent rate profile, we have performed the zeta potential measurement of CTAB alone and in the presence of DPA.

The zeta potentials of two sets of aqueous CTAB solutions with varying concentrations have been measured: the first set of surfactant solutions are free from DPA, while the second set of CTAB solutions are mixed with the same amount of DPA (Fig. 8). The positive zeta potential (ξ) value of CTAB alone in aqueous media is an indication of the cationic micellar surface

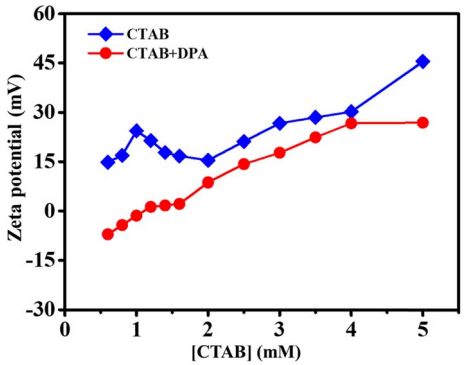

Fig. 8 Variation of the zeta potential with the concentration of CTAB in the presence of a fixed amount of DPA.

constituted by CTAB. An initial rise of zeta potential value with increasing CTAB concentration is observed; however, after reaching 1.0 mM [CTAB] the surface charge has been reduced (indeed positive ξ), and ultimately it approaches a constant. This concentration of CTAB (1.0 mM) should be marked as the micellization point, as evidenced from conductometric measurement also. After 2.0 mM, the ξ value increases steadily with the addition of CTAB, since a greater number of micelles are generated in the reaction medium.

The ξ value is markedly negative (−7.08 mV) in the presence of DPA at very low CTAB concentration (0.6 mM), which means the negatively charged silver(III) complex (DPA) contributes more to the surface charge of the pre-micellar aggregates. Without altering the [DPA], the increment of [CTAB] in solution showed a prominent rise in ξ value due to the intensification of positively charged species. The ξ value becomes unaltered in the range of [CTAB] 1.2 mM to 1.8 mM, indicating the substantial generation of aggregated nanostructures by which surface charge is balanced. A sharp increase in positive zeta potential value with respect to the [CTAB] was noticed from 1.8 mM to 4.0 mM, suggesting the fabrication of a greater number of aggregated nanostructures. Finally, no marked change in the surface charge is observed after 4.0 mM CTAB concentration. The shift of λ_{max} value to a higher wavelength supports the considerable interaction between the DPA molecules and CTAB

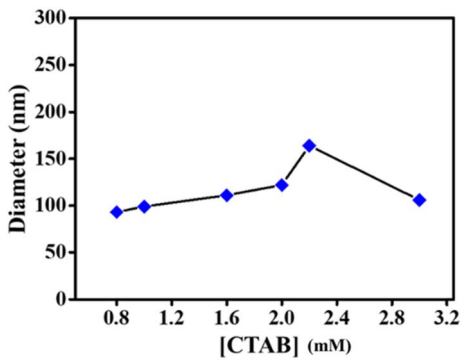

Fig. 9 Variation of the hydrodynamic diameter of the CTAB micellar aggregates in the presence of DPA.

nanoaggregates. The creation of a large number of hemimicelles or surfactant monolayers, as the consequence of such electrostatic interaction, causes the surface charge to gradually tend to be more positive with increasing CTAB concentration. Surface charge becomes highly positive close to the CMC (at 1.0 mM), showing the presence of a greater number of DPA complexes throughout the pre-micellar aggregations in the solution, which results in a higher rate at 0.8 mM CTAB.

However, the rates of oxidation for each of the alcohols intensifies following the generation of micelle-like definite nanoaggregates. It is noticed that for the oxidation of alcohols in a micellar-catalysed medium with DPA oxidant, propan-2-ol, exhibits a 40-fold, butan-2-ol exhibits a 15-fold, and pentan-2-ol exhibits a 15-fold rate increment compared to the reaction executed in aqueous media only. The variation in hydrodynamic diameter of the CTAB aggregates in the presence of DPA provides information regarding the affection of negatively charged DPA towards the positively charged micellar surface. The concentration of DPA is constant while the concentration of CTAB increases during the DLS measurement. From Fig. 9, we noticed that the CTAB starts to form a nano-dimensional aggregate around the 0.8 mM concentration range in the presence of [DPA]. The increase in reaction rate has been recognized at this concentration of CTAB on account of the aggregation made-up by CTAB of desirable size. Afterward, the hydrodynamic diameter of the CTAB nanoaggregates is augmented in the presence of DPA when the CTAB concentration increases gradually up to 2.2 mM due to the involvement of a large number of CTAB monomers in making the micelle-like aggregate. However, this outcome is a little bit contradictory in comparison to the earlier reports of micelle-mediated reaction kinetics, but the role of alcohols in decorating the micellar aggregates needs to be considered for clarification of the overall oxidation rate. Without further increment, the size of the nanoaggregate decreases at 3.0 mM concentration of CTAB. This could be the result of larger aggregates splitting into a greater number of smaller aggregates when the concentration of CTAB increases.

3.5. Mechanistic route of the studied reaction in a micellar microenvironment

As previously mentioned, the predominant periodate species in the alkaline medium is $[(H_3IO_6)_2]^-$. The OH^- deprotonates the DPA in the first equilibrium stage to produce a deprotonated diperiodatoargentate(III) that interacts with an alcohol molecule to generate an intermediate complex in the second equilibrium phase. The complex breaks down in a step that determines the rate of production of the products and Ag(I) species.[36] The products are characterised by the FTIR spectrum of its hydrazone derivatives (Fig. S1†). The overall mechanistic pathway of the reaction process is presented in Scheme 1 based on these experimental findings.

The catalysed route of oxidation can be demonstrated based on the concentration regions of CTAB, namely the pre-micellar, micellar, and post-micellar concentrations. The k_{obs} *vs.* [CTAB] plot (Fig. 7) illustrates the reaction rates of the studied reaction with varying CTAB concentration. The coulombic interaction between the negatively charged oxidant species and the positive micellar surface accounts for the increased rate constant value observed in the cationic CTAB micellar environment.[37] Because of the significant coulombic attraction, the concentrations of DPA molecules around the CTAB aggregates are higher than when the reaction proceeds without the surfactant-mediated reaction. In fact, the hydrophobic properties of alcohol molecules allow them to reside at the micelle's palisade layer, on the condition that the alcohols' –OH groups are orientated towards the micelle's stern layer (Scheme 2).[38] Therefore, the alcohol molecules could easily be oxidized by the oxidant. The rate of the reaction rises in the premicellar zone (0.6 mM to 0.8 mM range), as a result of the creation of premicellar aggregates.[39] k_{obs} (CTAB = 0.8 mM) > k_{obs} (CTAB = 2.0 mM) is explained on

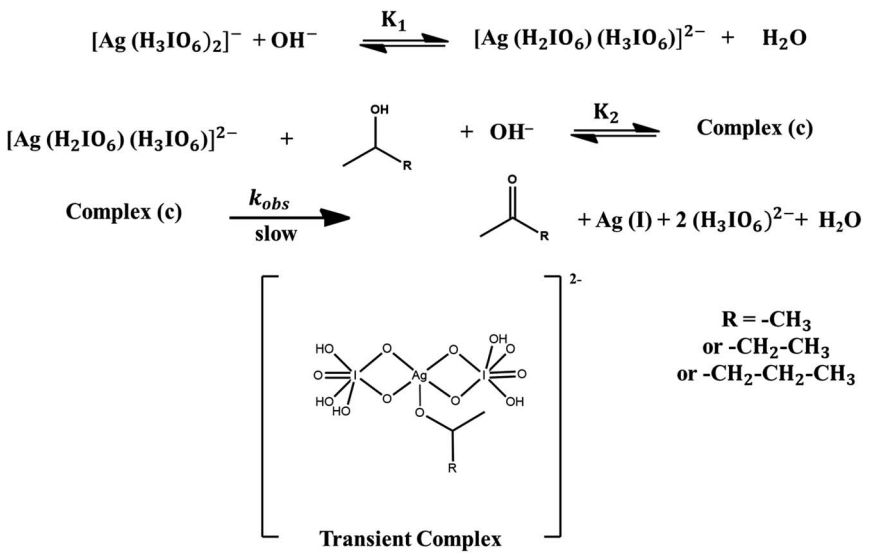

Scheme 1 Mechanistic pathway of the oxidation of homogeneous alcohols by DPA in aqueous alkaline medium.

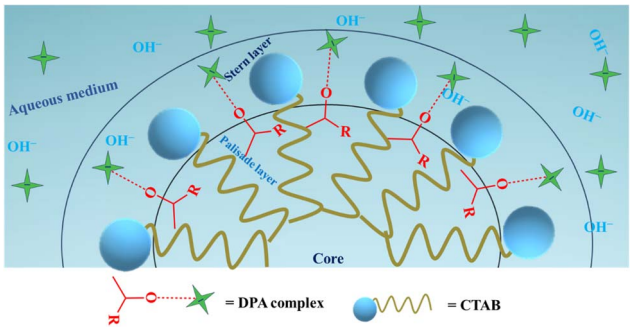

Scheme 2 Schematic representation of the distribution of reactant species in a micellar micro heterogeneous environment consisting of CTAB and DPA molecules.

the basis of the higher positive zeta potential value at 0.8 mM CTAB than 2.0 mM CTAB. This provides information on the increased quantity of negatively charged DPA molecules present on the micelle's outer surface at 0.8 mM CTAB. At a concentration of 2.0 mM CTAB, the rate constant of the reaction for all the substrates drops. After 2.0 mM CTAB concentration, the zeta potential of the micellar solution increases with increasing cationic CTAB concentration, which results in a higher rate constant associated with the corresponding CTAB concentration. The highest rate constants for all three alcohols are observed at a concentration of 5 mM CTAB (Fig. S7†).

4 Conclusion

The catalytic oxidation of aliphatic alcohols (mostly secondary) in a greener environment as fabricated by an aqueous CTAB surfactant is studied in detail. Employment of aqueous surfactant-micelles as the reaction medium energetically favours the oxidation and hence accelerates the reaction rate. The catalytic performance of micellar media is substantially investigated following the kinetics of oxidation at various CTAB concentrations. Interestingly, the mixture of DPA and CTAB produces a bathochromic shift of λ_{max} in the concentration range of 0.8 mM to 2.0 mM compared to the peak that appeared for aqueous DPA only; however, the λ_{max} value does not alter at [CTAB] > 2.0 mM. The favourable attraction between the positively charged premicellar surface and negatively charged DPA species plays the decisive role in order to develop such a bathochromic shift. The surface charge of the CTAB solution after CMC becomes extremely positive, indicating micelle development in shape. The stable nanoaggregate formation by the CTAB (after the reaching kinetic CMC) in the presence of substrate and oxidant ensues the significant increment of the reaction rate constant values. The localization of reactant molecules around the CTAB micellar surface promotes the collision frequency among the reactant species, which results in the ultimate catalytic rate enhancement. Surprisingly aqueous CTAB media produce maximum 40-fold rate enhancement for the oxidation of 2-propanol, while 15-fold increments were observed for the oxidation of the other two substrates. By probing the kinetic effects of CTAB surfactant media, this study reveals how CTAB surfactant media tune the reaction rates by compartmentalizing reactants within micellar microenvironments.

Data availability

Data will be made available on request.

Author contributions

All the authors have accepted responsibility for the entire content of this submitted manuscript and approved submission.

Conflicts of interest

The authors declare no conflicts of interest regarding this article.

Acknowledgements

SK, MM, SMR, and ML are thankful to the UGC, New Delhi for the Research Fellowship. PK is grateful to the CSIR, New Delhi for the Research Fellowship. In addition to expressing gratitude, the authors note that The University of Burdwan provided sufficient facilities and resources. For the instrumentation facilities, the authors are also grateful to IISER Kolkata.

References

1 P. T. Anastas and J. C. Warner, *Green Chemistry: Theory and Practice*, Oxford University Press: New York, 1998.
2 K. Hackl and W. Kunz, *C. R. Chim.*, 2018, **21**, 572–580.
3 B. H. Lipshutz, *J. Org. Chem.*, 2017, **82**, 2806–2816.
4 H. C. Hailes, *Org. Process Res. Dev.*, 2007, **11**, 114–120.
5 P. Sar and B. Saha, *Adv. Colloid Interface Sci.*, 2020, **284**, 102241.
6 P. Sar, A. Ghosh, A. Scarso and B. Saha, *Res. Chem. Intermed.*, 2019, **45**, 6021–6041.
7 G. L. Cohen and G. Atkinson, *Inorg. Chem.*, 1964, **3**, 1741–1743.
8 S. E. Leucuta, *Curr. Clin. Pharmacol.*, 2010, **5**(4), 257–280.
9 P. Makvandi, R. Jamaledin, M. Jabbari, N. Nikfarjam and A. Borzacchiello, *Dent. Mater.*, 2018, **34**(6), 851–867.
10 J. Y. Kim, J. K. Lee, T. S. Lee and W. H. Park, *Int. J. Biol. Macromol.*, 2003, **32**, 23–27.
11 A. Chakraborty, T. Chakraborty, M. I. Menendez and T. Chattopadhyay, *ACS Omega*, 2019, **4**(7), 11558–11565.
12 A. K. Das, A. Roy and B. Saha, *Transition Met. Chem.*, 2001, **26**, 630–637.
13 G. Kaur, K. Kaur and S. Handa, *Curr. Opin. Green Sustain. Chem.*, 2022, **38**, 100690.
14 J. R. Kincaid, M. J. Wong, N. Akporji, F. Gallou, D. M. Fialho and B. H. Lipshutz, *J. Am. Chem. Soc.*, 2023, **145**(7), 4266–4278.

15 R. Carpentier, W. Denis, F. S. Azcona, D. Carraro, G. Grauwels, M. Orlandi, C. Zonta, G. Licini and K. Bartik, *ACS Sustainable Chem. Eng.*, 2023, **11**(23), 8633–8641.
16 M. Layek, P. Karmakar, P. Pal, S. M. Rahaman, S. Kundu, M. Mitra, N. Khatun, M. Nandi, P. Sar and B. Saha, *Ind. Eng. Chem. Res.*, 2024, **63**(3), 1334–1348.
17 M. A. Malik and Z. Khan, *Colloids Surf., B*, 2009, **72**(2), 253–258.
18 S. Kundu, M. Layek, S. Mondal, M. Mitra, P. Karmakar, S. M. Rahaman, K. Mahali, A. Acharjee and B. Saha, *New J. Chem.*, 2024, **48**, 3804–3812.
19 A. Srivastava, M. K. Goswami, R. K. Dohare, N. Srivastava and K. Srivastava, *Int. J. Chem. Kinet.*, 2023, **55**(8), 431–440.
20 B. Chowdhury, P. Sar, D. Kumar and B. Saha, *J. Mol. Liq.*, 2022, **347**, 117993.
21 D. S. Munavalli, S. A. Chimatadar and S. T. Nandibewoor, *Ind. Eng. Chem. Res.*, 2007, **46**(5), 1459–1464.
22 A. T. Buddanavar and S. T. Nandibewoor, *Phys. Chem. Commun.*, 2016, **3**(2), 87–94.
23 S. Kundu, P. Karmakar, S. M. Rahaman, M. Mitra, S. Rajwar, S. Dhibar, M. Layek, P. Sar and B. Saha, *New J. Chem.*, 2023, **47**, 4364.
24 K. T. Sirsalmath, C. V. Hiremath and S. T. Nandibewoor, *Appl. Catal., A*, 2006, **305**, 79.
25 C. E. Crouthamel, H. V. Meek, D. S. Martin and C. V. Banks, *J. Am. Chem. Soc.*, 1949, **71**, 3031–3035.
26 D. G. Patil and S. T. Nandibewoor, *World J. Pharm. Res.*, 2015, **4**, 1219–1233.
27 P. Karmakar, S. Kundu, M. Layek, K. Karmakar, M. Mitra, A. Mukherjee, D. Dhak, U. Mandal, P. Sar and B. Saha, *New J. Chem.*, 2023, **47**, 13235–13246.
28 S. N. Yadav, S. Rai, P. Shah, N. Roy and A. Bhattarai, *J. Mol. Liq.*, 2022, **355**, 118949.
29 S. N. Yadav, S. Rai, A. Bhattarai and B. Sinha, *J. Mol. Liq.*, 2024, **399**, 124387.
30 M. T. Anderson, J. E. Martin, J. G. Odinek and P. P. Newcomer, *Chem. Mater.*, 1998, **10**(6), 1490–1500.
31 L. Wei, Z. Ming, Z. Jinli and H. Yongcai, *Front. Chem. China*, 2006, **1**, 438–442.
32 S. Das, S. Mondal and S. Ghosh, *J. Chem. Eng. Data*, 2013, **58**, 2586.
33 S. E. Moore, M. Mohareb, S. A. Moore and R. M. Palebu, *J. Colloid Interface Sci.*, 2006, **304**, 491–496.
34 C. A. Bunton and J. R. Moffatt, *J. Phys. Chem.*, 1986, **90**(4), 538–541.
35 M. R. Alavijeh, S. Javadian, H. Gharibi, M. Moradi, A. R. T. Bagha and A. A. Shahir, *Colloids Surf., A*, 2011, **380**(1–3), 119–127.
36 R. R. Hosamani and S. T. Nandibewoor, *J. Chem. Sci.*, 2009, **121**, 275–281.
37 A. Ghosh, K. Sengupta, R. Saha and B. Saha, *J. Mol. Liq.*, 2014, **198**, 369–380.
38 I. U. Nkole, S. Abdulsalam, I. Ibrahim and D. E. Arthur, *Chem. Afr.*, 2021, **4**, 525–533.
39 M. A. Malik, F. M. Al-Nowaiser, N. Ahmad and Z. Khan, *Int. J. Chem. Kinet.*, 2010, **42**(12), 704–712.